Electrically switchable diffraction grating using a hybrid liquid crystal and carbon nanotube-based nanophotonic device

Electrically switchable diffraction grating using a hybrid liquid crystal and carbon nanotube based nanophotonic device

Kanghee Won[1], Haider Butt[1], Ananta Palani[1], Philip J.W. Hands[2], Ranjith Rajeskharan[3], Qing Dai[1], Ammar Ahmed Khan[1], Gehan A. J. Amaratunga[1,4], Timothy D. Wilkinson[1]*

[1]*Department of Engineering, University of Cambridge, 9 JJ Thomson Avenue, Cambridge CB3 0FA, UK*
[2]*School of Engineering, The University of Edinburgh, The King's Buildings, Mayfield Road, Edinburgh, EH9 3JF, UK*
[3]*School of Physics, University of Melbourne, Victoria 3010, Australia*
[4]*Sri Lanka Institute of Nanotechnology (SLINTEC), Lot 14, Zone A, EPZ, Biyagama, Sri Lanka*
*Corresponding author: tdw13@cam.ac.uk

Abstract: We demonstrate a hybrid liquid crystal and carbon nanotube based device which shows the capacity to perform as a switchable diffraction grating. A liquid crystal layer was sandwiched between two electrodes (patterned into gratings). The bottom electrode consisted of a two dimensional square array of carbon nanotubes, while the top electrode comprised of an ITO based in-plane switching electrode on glass. The device displayed distinct voltage dependent diffraction patterns due to the two different electrodes. The diffraction patterns were studied both computationally and experimentally, with good agreement between the results obtained. Both the diffraction pattern and efficiency from the device could be switched by varying the applied voltage across the liquid crystal layer.

Keywords: Carbon nanotubes, in-plane switching, liquid crystals, electrically switchable, grating

Diffraction gratings are ideal candidates for the manipulation of optical beams (such as splitting and steering) in arbitrary controlled ways. Greater functionality is also possible by the development of electrically switchable diffraction gratings, using liquid crystals [1-5]. This paper presents a new and complex electrically switchable diffraction grating device, based upon the recently reported nanophotonic technology of using carbon nanotubes (CNTs) as electrode structures in liquid crystal (LC) devices [6]. Such hybrid LC-CNT technology has also recently been demonstrated in the form of adaptive cylindrical [7] and spherical [8] microlens arrays with

low switching voltages, and as an invaluable tool for integral field imaging techniques for 3D microscopy [9].

So far we have demonstrated nanophotonic devices based on the hybrid combination of LC and carbon nanotubes, which utilize the near field focusing and lensing effects. Here we study the far-field diffraction effects from such devices. We demonstrate that hybrid LC-CNT technology not only shows great potential for near field refractive optical devices, but also for diffractive applications, including tunable gratings and beam steering. We present the fabrication and characterization of an electrically switchable diffraction grating using a hybrid LC-CNT nanophotonic device with an in-plane switching electrode (IPS). The resulting diffraction patterns were investigated both computationally and experimentally. A good agreement between the theoretical and measured results was achieved.

To fabricate the electro-optical device a liquid crystal cell was assembled using two special substrates. These substrates acted as electrodes for addressing the LC layer sandwiched between them. The top substrate consisted of glass with an interdigitated pattern of two indium tin oxide (ITO) electrodes, as shown in Fig. 1(a). The interdigitated electrodes address the LC layer acting as an in-plane switching (IPS) structure. The second (lower) electrode consisted of an array of multiwall carbon nanotubes (MWCNTs) fabricated on an opaque silicon substrate. The array of MWCNTs, with an average tube diameter of 50 nm and height of 2 μm, was patterned on silicon substrate using the standard plasma enhanced chemical vapour deposition process, fully explained in our previous paper [6]. To make all the nanotubes a common electrode, the nanotube array was coated with aluminium. Due to aluminium coating the bottom electrode was reflective and the device operated in reflecting mode.

A polyimide (AM4276 from Merck) was applied to the patterned ITO coated upper glass substrate and rubbed to provide homogeneous planar LC alignment. The two substrates were then glued together with an optically curable adhesive (Norland NOA68) mixed together with spacer beads (Merck), which provided a uniform cell thickness of 20 μm. Electrical wire connections were made to the two substrates using indium solder. Two connections were made to the top IPS electrodes and one connection to the bottom MWCNT array. The schematic diagram of the fabricated device is shown in Fig. 1(c).

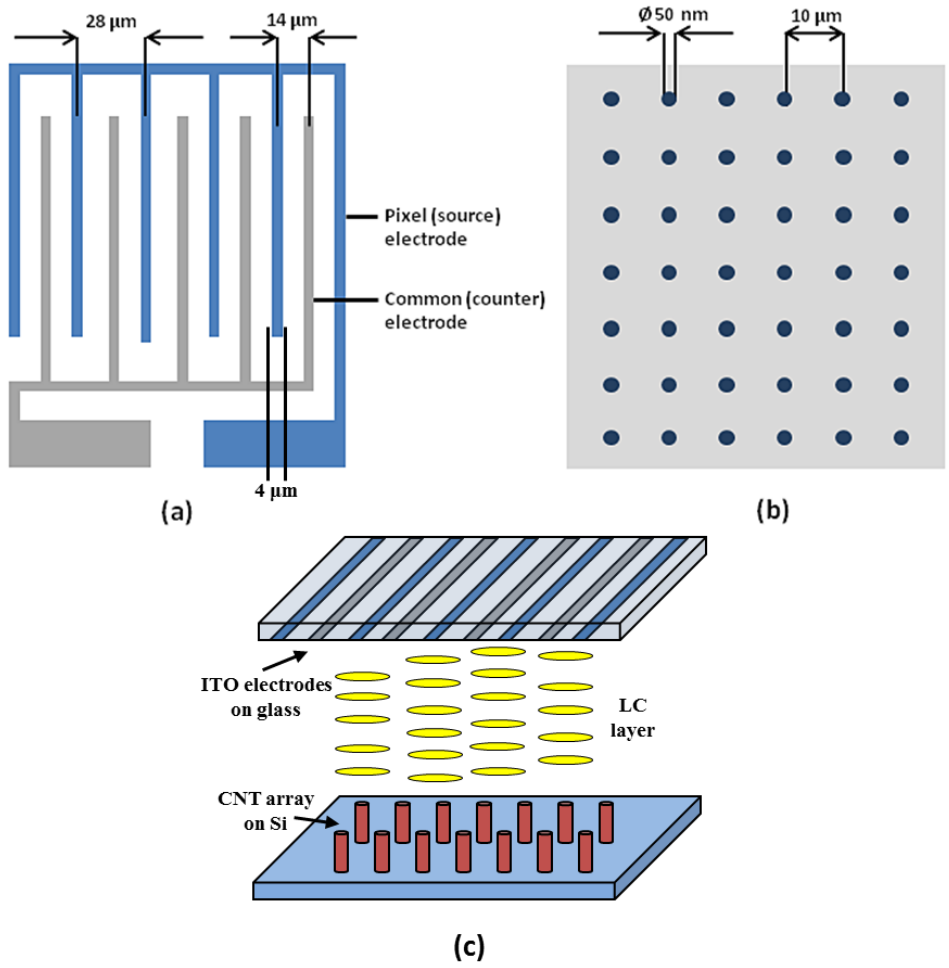

Fig. 1. Structure of (a) interdigitated ITO electrodes and (b) MWCNT array on silicon substrate. (c) Schematic diagram of the fabricated hybrid liquid crystal and carbon nanotube based photonic device.

Due to fabrication limitations there was a mismatch between the periodicities of the two electrodes. The periodicity of ITO IPS electrode was 14 µm, while the periodicity of the square lattice nanotube array was 10 µm. Also, because of the nanoscale dimensions of the carbon nanotubes it was difficult to exactly align the bottom nanotube rows with the rows of ITO in the top IPS electrode.

The electric fields produced by these two electrodes address the LC layer and dictate the molecular arrangements. To understand the effective electric field produced with in the device by these two electrodes, finite element method (FEM) modelling was performed. The modelling of

static electric fields was perfumed in response to the DC voltages. Fig. 2(a) shows the modelled geometry of the device. Alternative voltages were applied to the top IPS electrode while the bottom CNT electrode was set to ground. Fig. 2(b) and (c) show the potential profile across the device and the resultant electric fields produced. The nanotubes produce strong localised electric fields due to their high aspect ratios, distorting the vertical electric field produced by the lower planar electrode.

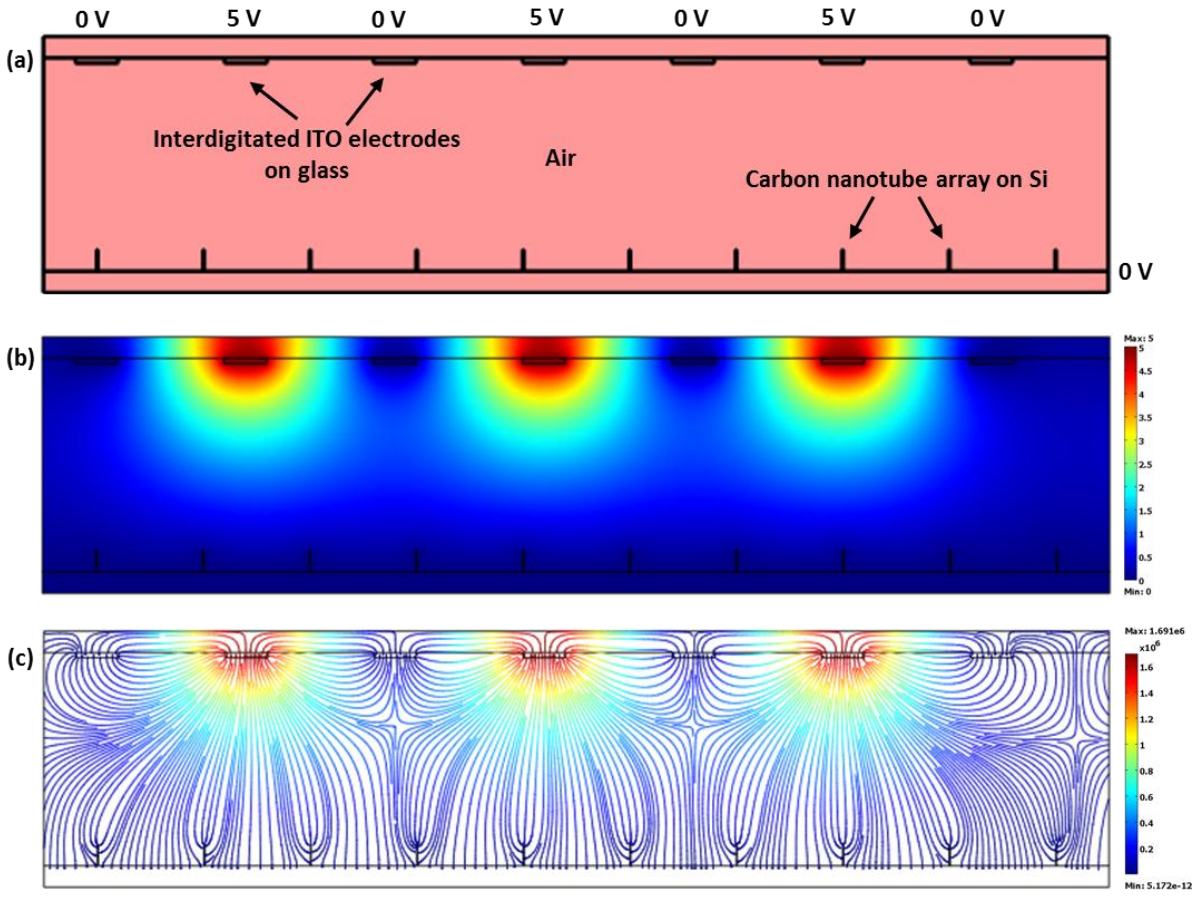

Fig. 2. (a) Modelled device geometry used to simulate the static electric fields. (b) The electric potential profile within the device. (b) Simulated resultant electric field produced by the two electrodes.

The IPS electrode on the other hand (due to the alternative voltages) produces curved electric fields. As shown in Fig. 2(c) a cylindrical electric field profile is produced around any three neighbouring ITO electrodes, with a grounded ITO electrode in the centre. This field profile

covers a wider area in the device as compared to the fields produced by nanotubes. This electric field also dictates a cylindrical index profile within the LC layer producing an array of LC based lenticular lenses, as reported previously [7]. The phase profile of these lenticular lenses was voltage dependent.

A theoretical diffraction simulation of the nanophotonic device was also performed. The simulated device consisted of two periodic gratings present on the two electrodes, with liquid crystal as the tunable media. The expected diffraction pattern produced by each of the gratings was computed using Fourier analysis. With ITO electrode being optically transparent, with no voltage applied the carbon nanotube grating is the only dominant grating modulating the propagation of light causing diffraction. The carbon nanotube array was modeled as a 2D binary intensity grating of approximately circular spots. Fast Fourier transform (FFT) of the grating revealed the far-field diffraction pattern produced from it, as shown in Fig. 3(a-c). The simulated FFT displayed a square grid of discrete intensity spots, with a strong central zero order consisting of undiffracted light. Log plots of the FFT were performed to suppress the zero order and to help show the higher orders in the diffraction pattern more visibly. Due to the circular shape of the nanotubes (aperture) a circular envelope was observed over the calculated diffraction pattern, clearly visible in the 3D plot of Fig. 3(c).

Next, the optical diffraction patterns from the device with various voltages applied were calculated. At non-zero voltages, the IPS electrodes address the LC layer producing a phase grating of lenticular lenses. The device offers two gratings to the incident light, the nanotube arrays and the lenticular lens array. The voltage dependent phase profile induced by these lenses was reported in [7]. These profiles (also shown in supplementary material) were used to model the grating for Fourier analysis. As shown in Fig. 3(d-f), at 2 volts peak-to-peak (V_{pp}) the nanophotonic device was modeled as a combination of the 2D binary amplitude grating (due to the CNT array) and a superimposed phase grating (due to the LC lenticular lenses). The FFT was calculated to determine the diffraction pattern of the combined grating. The diffraction pattern displayed a horizontal spreading of the intensity. Since the lenticular lenses have a smaller dimension in the horizontal direction, the diffraction pattern displays a larger horizontal dimension as expected.

Fig. 3(g-i) and 3(j-l) display the calculated results at 4 and 6 V_{pp} respectively. With increasing voltage, the lenticular lenses become broader while also exhibiting increased peak phase modulation. The lenses cover a larger portion of the device as compared to the nanotube array. Therefore, at higher voltages the FFT shows a horizontally extended pattern with most of the light localized in the central horizontal row.

The simulated results show that by varying the voltage applied to the IPS electrode, the diffraction pattern displayed by the device can be modified. With no voltage applied the device displays a square grid diffraction pattern. As voltage is increased, when the LCs are fully switched the device displays diffraction patterns expected from an array of lenticular lens. This is of interest as this proves that the device can act as a tunable grating which can be utilized for applications like waveguide couplers and optical switches.

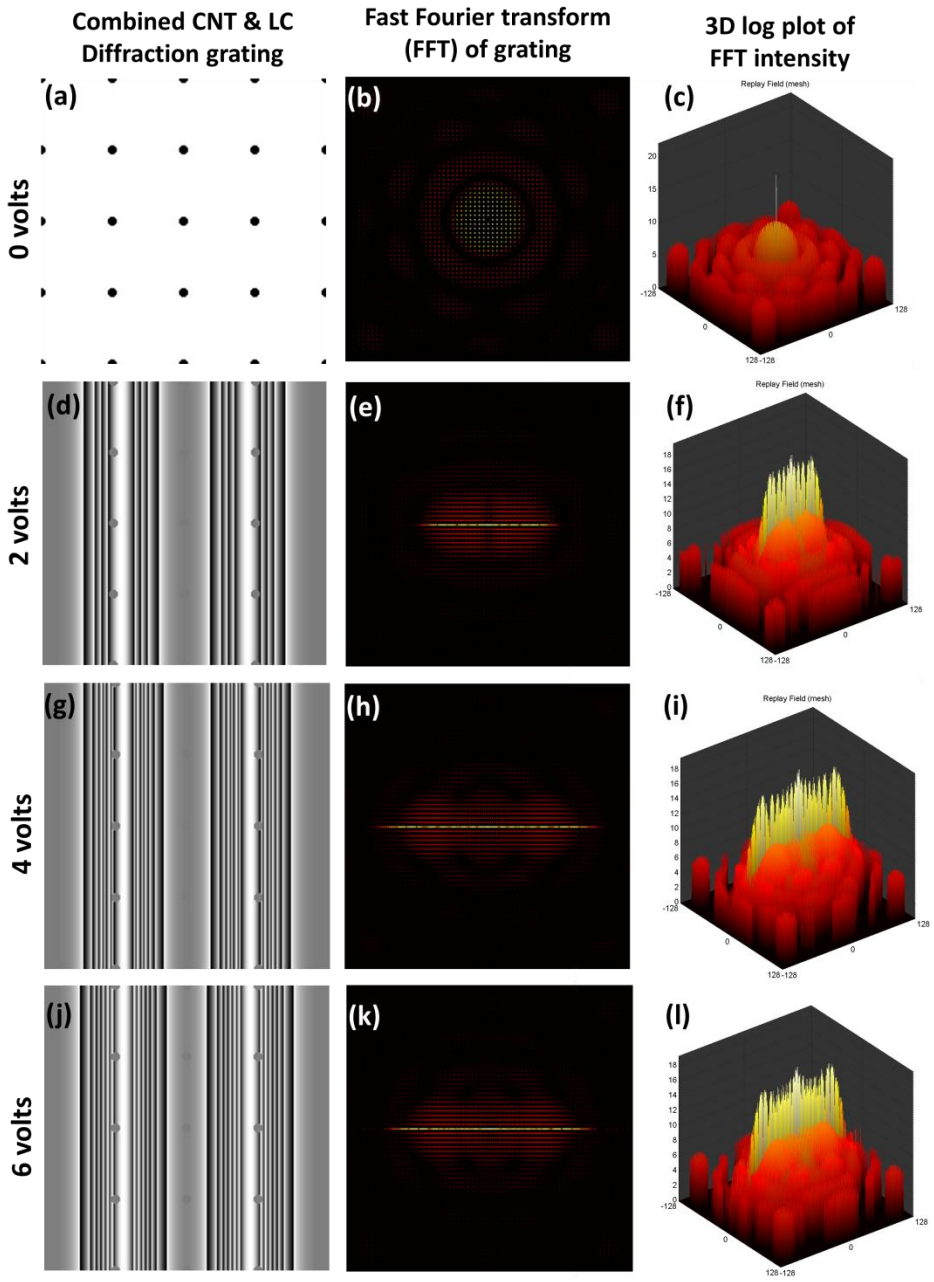

Fig. 3. (a) Simulated carbon nanotube array grating. Log plot of diffraction pattern from the CNT array in (b) 2D and (c) 3D view. Combined gratings consisting of CNT array and phase array of LC lenticular lenses at (d) 2, (g) 4, and (j) 6 volts V_{pp}. Simulated diffraction patterns of the same in (e, h, k) 2D and (f, i, l) 3D view.

The far-field diffraction patterns from the hybrid LC-CNT device were experimentally obtained. A He-Ne laser beam (λ = 633 nm) was used as a light source to illuminate the device. The

incident laser light was reflected from the device, after having interacted with both the gratings. The reflected light was collected onto a screen placed about 20 cm away and was also measured with an optical energy meter. Alternating current (AC) voltages (at 1000 Hz) were then applied across the electrodes. One of the top IPS electrodes and the bottom CNT electrode were connected to ground, while voltage was applied to the other IPS electrode. The resulting voltage dependant diffraction patterns are shown in Fig. 4.

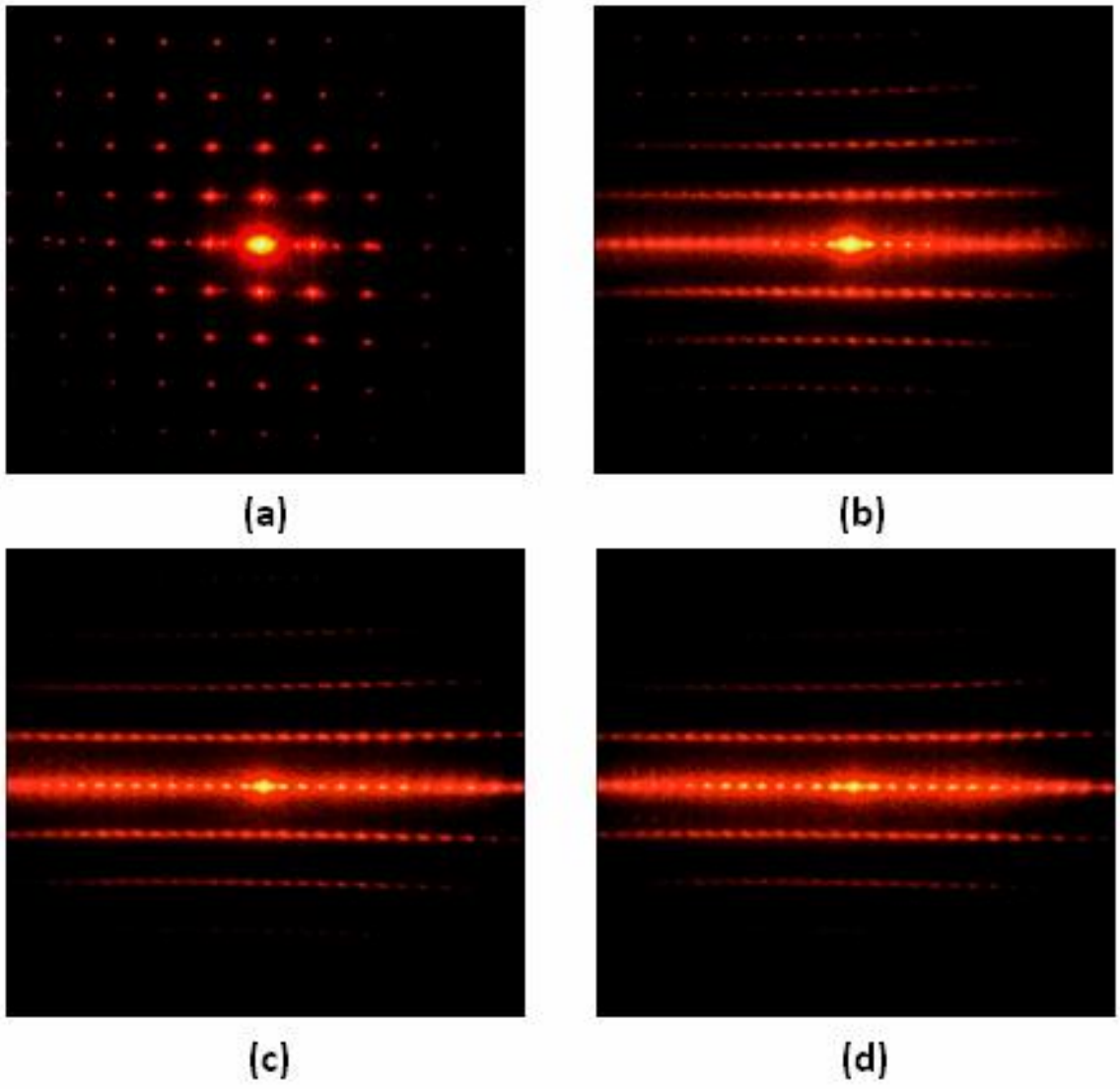

Fig. 4. The diffraction patterns arising from a hybrid LC-CNT device with LC layer switching at four different voltages (a) 0, (b) 2, (c) 4, and (d) 6 V_{pp}.

At zero V_{pp}, in the absence of an electric field, the liquid crystals are mostly horizontally aligned and do not show any switching. As the ITO is mostly transparent, the most prominent feature observed by the incident light is the MWCNT array based grating. Each nanotube acts as a defect within the LC layer creating a distorted molecular arrangement around it. The incident light is diffracted by the square array of LC defects produced by the MWCNT array. As shown in Fig. 4(a), at zero V_{pp} the pattern consists of a square grid of diffracted spots which matches very closely with the simulated diffraction pattern for the square MWCNT array. As the applied voltage to one of the IPS electrodes is increased, a curved electric field is produced within the device as predicted by the FEM modelled result in Fig. 2. This electric field addresses the liquid crystal molecules near the top electrode causing the formation of periodic graded index cylindrical rows with in the liquid crystal layer. When a potential difference beyond the Freedrickzs transition (at 2 V_{pp}) was applied across the cell, the diffraction pattern from the device changed.

At a voltage of around 2 V_{pp}, when LC molecules start switching, rows seem to form in the diffraction pattern, with the zero-order splitting into further orders (Fig. 4(b)). More diffracted spots appear horizontally within the rows of the square grid, increasing the horizontal density of spots. The light localization and intensity distribution increases within the rows. The overall diffraction pattern is observed to change from the square grid (predicted for the nanotube array) to the stack of horizontal rows. When the voltage is further increased from 4 to 6 V_{pp} (Fig. 4(c-d)) the LC molecules completely switch and the intensity of the middle row increases. This is the predicted feature of the diffraction pattern from the 1D grating of lenticular lenses, presented in Fig. 3 (k-m). This shows that with an increase in voltage the influence of the top interdigitated ITO electrodes increases within the LC layers. The diffraction pattern switches from the square grid (at zero V_{pp}) to a dominant row in the middle of the pattern (perpendicular to the IPS electrodes). A good match was achieved between the simulations and measurements.

The diffraction efficiency (DE) of a hybrid LC-CNT device was measured using a polarized laser and power meter. The vertically aligned carbon nanotubes have an anisotropic structure and display a polarization and angle dependent interaction with light. Also, the top IPS electrode was one dimensional. Therefore, it was of interest to study the diffraction efficiency of the device with respect to different polarizations, incident angles, and voltages. A schematic diagram of the

experiment used to measure the DE is shown in Fig. 5(a). The device efficiency was measured for two polarizations of light, transverse magnetic (TM) and transvers electric (TE), as presented in Fig. 5(b-c). The diffraction efficiency was calculated using the equation DE = $(I - I_o)/ I$, where I_o is the intensity of zero order (undiffracted light) and I is the intensity of the incident laser beam [10].

At zero V_{pp} the device displays a DE of about 38% at zero degrees incident angle for both polarizations. At this voltage the nanotube grating is the dominant cause of diffraction. The zero incident angles the nanotubes show polarization independence. However as the incident angle increases the CNT area exposed to light increases, which increases the amount of light diffracted. Due to this reason the DE increases at zero V_{pp} with an increase in angle. Likewise, as 1 V_{pp} very similar behavior is observed showing that the LCs have not switched.

At a voltage of 2 V_{pp}, which is equivalent to the threshold voltage of LC molecules, an increase in DE is observed. In the device the LC phase grating is switched with different applied voltages which cause the light distribution between the orders to change and the intensity of each order to vary. At 3 V_{pp} a DE of about 50% is observed at zero degrees incident angle for both polarizations. At higher voltages the lenticular lens grating dictated by the IPS electrodes within the LC layer is more dominant. This phase grating encompasses a larger area as compared to the nanotubes and thus causes large scale phase perturbations in the LC layer. Therefore, at higher voltages the diffracting elements occupy a larger area which allows more light to be diffracted and drastic increase in efficiency is observed.

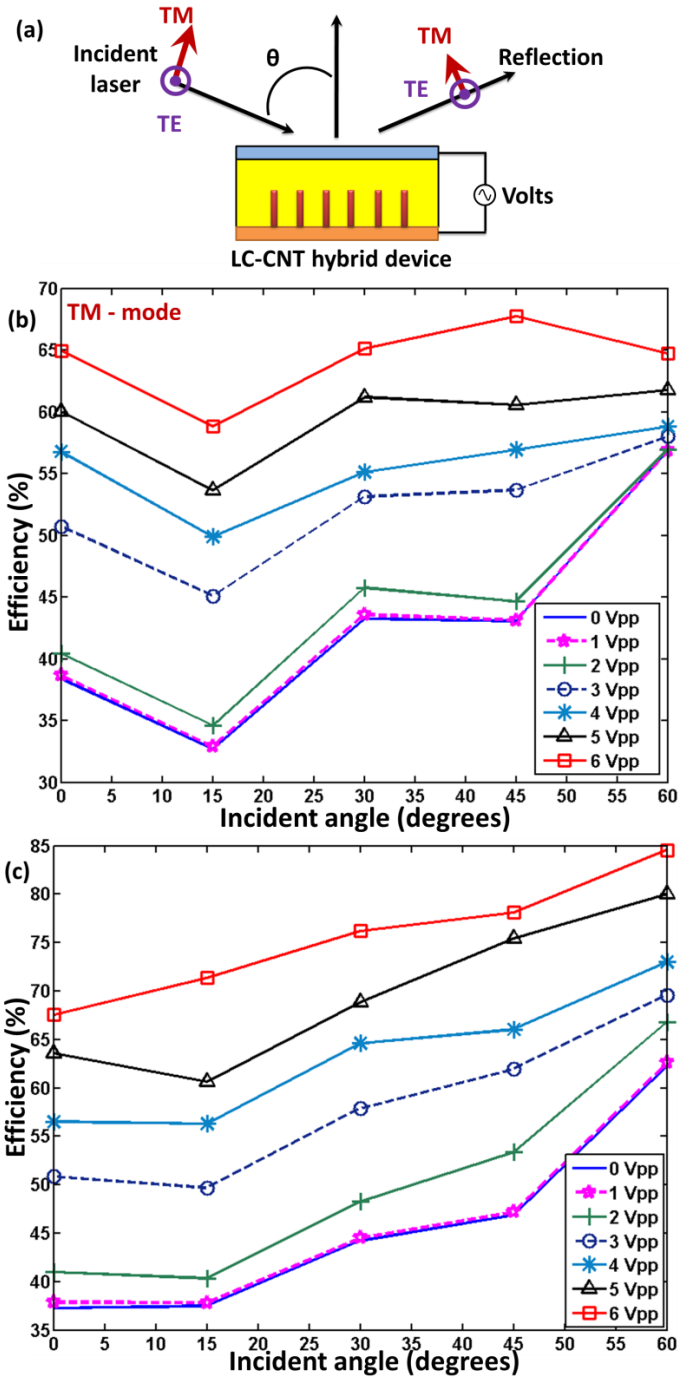

Fig. 5. (a) Schematic diagram of the experiment used to measure the device diffraction efficiency. Measured efficiency with varying incident angles and voltages for (b) TM-mode and (c) TE-mode polarization of light.

For TM mode polarized light, incident angle independence is observed for higher voltages (from 3 to 6 V_{pp}). With the increase in incidence angle the DE remains approximately consistent with a highest DE of about 67% at 6 V_{pp} and a 45 degree angle of incidence. However, for the TE mode polarized light, even at higher voltages the efficiency increases with the increase in incidence angle of the laser. This could be due to the increased area interaction of TE polarized light with the lenticular lenses (which are parallel to the TE polarization of laser). The highest observed efficiency of about 85% is observed at a voltage of 6 V_{pp} and 60 degrees incidence angle.

In conclusion, we have demonstrated an electrically switchable diffraction grating that consists of a nanotube array and an ITO based IPS electrode structure with nematic liquid crystal. Distinct and voltage dependent diffraction patterns are produced by the nanotube array and the IPS electrode addressed LC phase grating. The diffraction patterns were simulated using Fourier analysis and were later experimentally verified, with good agreement. The diffraction effects from the two electrode gratings can be electrically switched, which changes the diffraction pattern and diffraction efficiency. Such nanophotonic devices are very suitable for applications like tunable gratings and optical switches.

References

[1] R. Caputo, L. De Sio, A. Veltri, and C. Umeton, "Development of a new kind of switchable holographic grating made of liquid-crystal films separated by slices of polymeric material," *Optics Letters,* vol. 29, pp. 1261-1263, Jun 1 2004.

[2] J. Chen, P. J. Bos, H. Vithana, and D. L. Johnson, "An Electrooptically Controlled Liquid-Crystal Diffraction Grating," *Applied Physics Letters,* vol. 67, pp. 2588-2590, Oct 30 1995.

[3] J. Zhang, V. Ostroverkhov, K. D. Singer, V. Reshetnyak, and Y. Reznikov, "Electrically controlled surface diffraction gratings in nematic liquid crystals," *Optics Letters,* vol. 25, pp. 414-416, Mar 15 2000.

[4] C. Provenzano, P. Pagliusi, and G. Cipparrone, "Highly efficient liquid crystal based diffraction grating induced by polarization holograms at the aligning surfaces," *Applied Physics Letters,* vol. 89, pp. -, Sep 18 2006.

[5] R. Rajasekharan, C. Bay, Q. Dai, J. Freeman, and T. D. Wilkinson, "Electrically reconfigurable nanophotonic hybrid grating lens array," *Applied Physics Letters,* vol. 96, pp. -, Jun 7 2010.

[6] T. D. Wilkinson, X. Wang, K. B. K. Teo, and W. I. Milne, "Sparse Multiwall Carbon Nanotube Electrode Arrays for Liquid-Crystal Photonic Devices," *Advanced Materials,* vol. 20, pp. 363-366, 2008.

[7] K. Won, R. Rajasekharan, P. Hands, Q. Dai, and T. D. Wilkinson, "Adaptive lenticular lens array using a hybrid liquid crystal--carbon nanotube nanophotonic device," *Optical Engineering,* vol. 50, pp. 054002-6.

[8] R. Rajasekharan-Unnithan, H. Butt, and T. D. Wilkinson, "Optical phase modulation using a hybrid carbon nanotube-liquid-crystal nanophotonic device," *Opt. Lett.,* vol. 34, pp. 1237-1239, 2009.

[9] R. Rajasekharan, T. D. Wilkinson, P. J. W. Hands, and Q. Dai, "Nanophotonic Three-Dimensional Microscope," *Nano Letters,* vol. 11, pp. 2770-2773, 2012/05/30.

[10] M. D. Fayer, "Dynamics of Molecules in Condensed Phases - Picosecond Holographic Grating Experiments," *Annual Review of Physical Chemistry,* vol. 33, pp. 63-87, 1982.